JOM, Vol. 73, No. 2, 2021
https://doi.org/10.1007/s11837-020-04449-1

Thermo-mechanical Characterization of an Aged $Ni_{45.3}Ti_{39.7}Hf_{10}Pd_5$ Shape Memory Alloy

E. ACAR,[1,5] G.P. TOKER,[2] S. SAEDI,[3] H. TOBE,[4] and H.E. KARACA[2]

1.—Department of Aeronautical Engineering, Erciyes University, 38039 Melikgazi, Kayseri, Turkey. 2.—Department of Mechanical Engineering, University of Kentucky, Lexington, KY 40506, USA. 3.—Department of Systems Engineering, University of Arkansas at Little Rock, Little Rock, AR, USA. 4.—Institute of Space and Astronautical Sciences, Kanagawa 252-5210, Japan. 5.—e-mail: emreacar@erciyes.edu.tr

Thermo-mechanical characterization of a $Ni_{45.3}Ti_{39.7}Hf_{10}Pd_5$ polycrystalline shape memory alloy after aging at 550°C for 3 h was conducted. Thermal cycling under constant stress, superelasticity and loading till failure tests were employed to reveal the shape memory and material properties. Recoverable shape memory strain of 3.8% was achieved under compressive stress of 500 MPa. The sample showed almost perfect superelasticity above 70°C with total recoverable strain of about 4%, but failed at 2340 MPa with compressive strain > 13% at 35°C, and aging was not found to significantly affect its shape memory behavior because of the low volume fraction of precipitates.

INTRODUCTION

In the last decade, the research on shape memory alloys (SMA) has enabled significant improvements owing to their distinct behaviors such as the shape memory effect and superelasticity.[1] The shape memory effect is the shape recovery ability driven by heating after deformation in the martensitic phase, and superelasticity is the reversible shape change upon unloading after loading in austenitic phase.[1] NiTi-based shape memory alloys are the most studied system leading to their use in many current applications.

NiTi alloys have some drawbacks that need to be addressed before their use in applications (e.g., the aerospace, oil–gas, automotive and energy fields), which require high-temperature and high-strength capabilities. These weaknesses include low transformation temperatures (TTs) < 100°C, low dimensional stability and low strength.[2] Thus, many methods such as aging, alloying and processing techniques have been employed to mitigate these limitations.[1,3] Among these methods, alloying has been determined to be a very effective tool in increasing the TTs of NiTi[2] alloys. Alloying additions such as Hf, Pt, Pd, Au, Cu, Fe and Zr have been the most frequently used elements for this purpose.[2] Of these elements, Hf has been the most promising addition due to its lower cost and greater effectiveness in increasing TTs.[2] It was reported that the TTs of NiTiHf alloys could reach up to 525°C when 30% Hf was added at the expense of Ti in NiTi.[4,5] Thus, NiTiHf alloys have emerged as one of the most promising candidates for high-temperature SMA applications.

However, few challenges remain to be solved before NiTiHf SMAs can be practically used. These challenges are the low ductility, high density and low compatibility between the transforming phases due to Hf addition.[2,6] In addition to these, Ni-lean NiTiHf alloys suffer from poor strength because of the low critical shear stress (CSS) for dislocation slip, specifically at high temperatures. Due to the low CSS, residual strain is observed as a consequence of both plasticity and martensitic transformation. Therefore, the CSS levels should be increased to improve the shape memory behavior of NiTiHf alloys.[7]

One of the powerful ways to improve the shape memory properties of NiTiHf alloys is quaternary alloying.[6] Five alloying elements such as Cu, Pd, Zr, Nb and Sc have been added to NiTiHf.[8–12] Among these alloying additions, the NiTiHfPd alloy system has been found to be promising because of its high strength, high damping capacity and adjustable TTs.[13,14]

(Received April 30, 2020; accepted October 16, 2020; published online November 4, 2020)

Single-crystal and polycrystalline NiTiHfPd alloys have been investigated through thermo-mechanical experiments.[8,15–19] It was found that single-crystal alloys can show huge stress hysteresis > 1200 MPa under compressive stress levels of 2.5 GPa along the [111] orientation. On the other hand, shape memory strain of almost 2% was realized against a compressive stress of 1.5 GPa. It was observed that aging of NiTiHfPd alloys introduced (Ni + Pd)-rich precipitates after proper treatments, and aging was found to be very effective in tailoring shape memory properties such as TTs, transformation strain, strength and hysteresis. However, most of the above-mentioned studies have been conducted on $Ni_{45,3}Ti_{29,7}Hf_{20}Pd_5$ alloys. Thus, studies on the effect of stoichiometry alteration among NiTiHfPd alloys are limited.

Hf content in most of the previously studied NiTiHfPd alloys was 20 at.%.[6] Understanding the full promise of NiTiHfPd alloys requires further experimental and theoretical considerations using various chemical compositions and heat treatments. Previously as-received $Ni_{45.3}Ti_{39.7}Hf_{10}Pd_5$ polycrystalline alloys were investigated under compressive stresses.[6] The as-received alloy showed reasonable shape memory responses with 4.6% transformation strain under 500 MPa. A nearly complete superelastic response with 7% applied strain and > 4% transformation strain at 90°C under a stress level of 1250 MPa was also achieved. In this study, the shape memory behavior of the same $Ni_{45.3}Ti_{39.7}Hf_{10}Pd_5$ polycrystalline alloys was thermo-mechanically characterized after aging at 550°C for 3 h. The main aim is to investigate whether aging can alter and improve the shape memory behavior of these alloys.

EXPERIMENTAL PROCEDURE

An arc melting technique was used to produce a $Ni_{45.3}Ti_{39.7}Hf_{10}Pd_5$ (at.%) polycrystalline alloy ingot using high-purity elements [99.98 wt.% Ni, 99.95 wt.% Ti, 99.7 wt.% Hf (excluding Zr) and 99.99 wt.% Pd], which were procured from Alfa Aesar, USA. The melted ingot was homogenized at 900°C for 72 h in a vacuum followed by a furnace cooling process. A KNUTH electro-discharge machine (EDM) was used to produce samples (8 mm long and 4 × 4 mm^2 cross section) for compression tests. The compression samples were re-homogenized at 1050°C for 4 h followed by water quenching to ensure a homogeneous microstructure. Following the homogenization process, specimens were aged at 550°C for 3 h in air atmosphere and then quenched in water. The aged material will be called "aged NiTiPd-10Hf" throughout the article for brevity. Mechanical tests were conducted using a 100 kN MTS Landmark servohydraulic test platform. A 12-mm-guage length MTS extensometer was utilized to measure strain. Constant stress thermal cycling experiments were performed with a heating/cooling rate of 10°C/min. In the constant-temperature loading experiments, the loading strain rate was 8×10^{-4}/s while the unloading force rate was 100 N/s. Transmission electron microscopy (TEM) measurements were carried out using a JEOL 2010F instrument run at 200 kV. The TEM specimens were prepared by twin-jet polishing in a solution with chemical compositions of 20% H_2SO_4 and 80% CH_3OH.

RESULTS AND DISCUSSION

Figure 1 shows the bright-field TEM images of the aged NiTiPd-10Hf polycrystalline alloy. The images show the formation of $B19^{'}$ martensitic structure. Martensite plates with 20–50 nm thickness are visible in the images. In addition to martensite plates, nano-sized (40–50 nm) precipitates formed after aging. The volume fraction of precipitates in this study was determined to be lower than the ones observed in the $Ni_{50.3}Ti_{29.7}Hf_{20}$[20] and $Ni_{45.3}Ti_{29.7}Hf_{20}Pd_5$ alloys.[16] It is widely accepted that Ni-rich precipitates have utmost importance in altering mechanical (e.g., strength) and shape memory properties (e.g., strain, TTs, etc.) of NiTi- and NiTiHf-based alloys.[1,21] The high-volume fraction of Ni-rich precipitates can increase the strength and stabilize the shape memory behavior in NiTi- and NiTiHf-based alloys. Precipitates are also effective in altering TTs of NiTiHfPd alloys.[13,14] Thus, the low-volume fraction of precipitates in the current material might result in only minor changes in the strength and shape memory properties as was previously observed in $Ni_{45.3}Ti_{39.7}Hf_{10}Cu_5$ (at.%) polycrystalline alloys.[9]

The constant-stress thermal cycling responses of the aged NiTiPd-10Hf alloy is shown in Fig. 2. The samples were thermally cycled under selected compressive stresses between the temperatures above the austenite finish (A_f) and below the martensite finish (M_f) temperatures. The applied stress was incrementally increased, and the thermal cycling procedure was repeated. Figure 2 shows that TTs increased with stress. The M_s temperatures were 35°C and 87°C under 100 MPa and 700 MPa, respectively, while they were 16°C and 78°C under 100 MPa and 700 MPa, respectively, in as-received condition.[17] It is evident that the TTs after aging are slightly higher than the as-received condition. The higher TTs can be linked to the formation of precipitates upon aging, since it is known that H-precipitates in the NiTiHf-based alloys increase the TTs.[2]

Figure 3a shows the recoverable strain of aged NiTiPd-10Hf as a function of the applied stress (extracted from Fig. 2). The recoverable strains (transformation strain-irrecoverable strain) were 0.7% and 3.6% at 100 MPa and 700 MPa, respectively. The recoverable strain increased to 3.8% with stress till 500 MPa and then decreased to 3.6% at 700 MPa. The increase in the recoverable strain

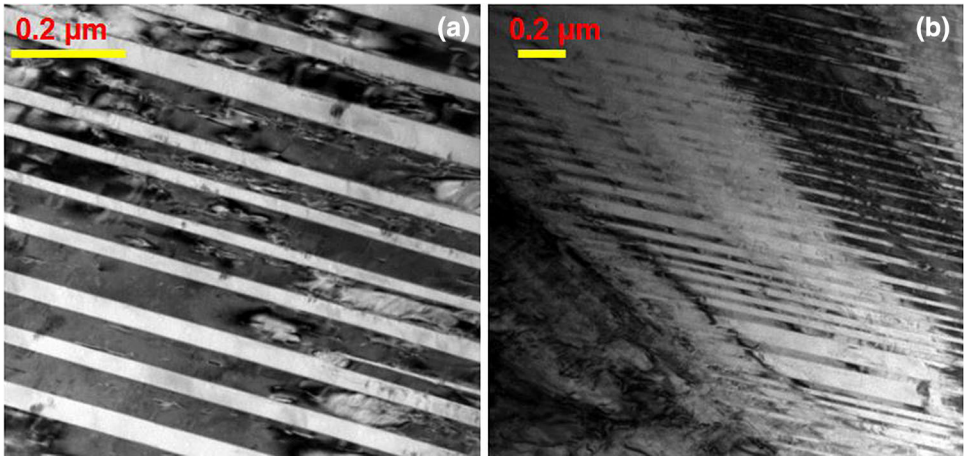

Fig. 1. (a) Bright-field TEM micrograph showing martensite plates and precipitates and (b) bright-field TEM micrograph showing a broader area of the aged NiTiPd-10Hf polycrystalline shape memory alloy.

stems from the widely known fact that martensite variants are favored at the expense of others because of the application of higher external stress. As the external stress increases, the amount of orientated martensite variants increases. At high stress levels, plastic deformation might occur simultaneously to martensite reorientation, and this results in retained martensite. Consequently, the volume fraction of the material that can undergo phase transformation[22,23] decreases. This results in a decrease in recoverable strain as shown for 700 MPa in Fig. 3a. The maximum recoverable strain level is lower compared to the as-fabricated NiTiPd-10Hf alloy with a maximum recoverable strain of 4.6% under 500 MPa. It is clear that aging resulted in a decrease in the maximum recoverable strain level in the NiTiPd-10Hf alloy. Since the precipitates do not undergo phase transformation, the amount of transformable materials decreases with aging, and this causes the recoverable strain to decrease. Another factor can be attributed to the changes in martensite morphology with aging.

Figure 3b shows irrecoverable strain and thermal hysteresis as a function of applied stress. The thermal hysteresis was measured at the mid-point of the transformation strain between cooling-heating curves (Fig. 2) by a graphical method. The thermal hysteresis under 100 MPa was 66°C, and it increased to 95°C at 700 MPa. On the other hand, there was no observable irrecoverable strain up to 300 MPa while it was 0.9% at 700 MPa. It is clear that as the externally applied stress increased, irrecoverable strain was also increased because of plastic deformation. It is also clear that the thermal hysteresis increases linearly with the applied stress. It is widely accepted that hysteresis in shape memory alloys is closely linked to the energy dissipation during phase transformation. These dissipations might include friction between martensite and austenite and interaction of martensite variants with themselves and precipitates.[8,24,25]

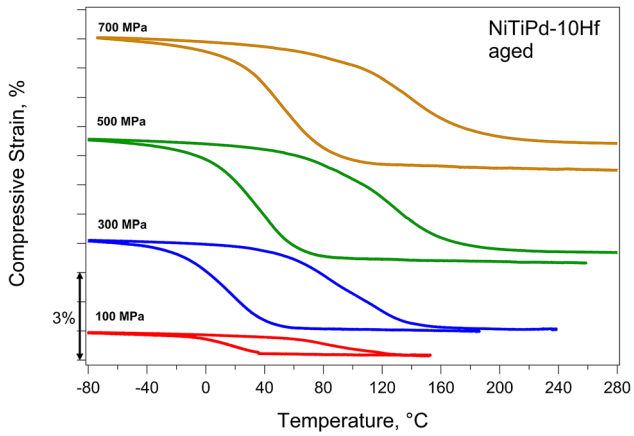

Fig. 2. Constant-stress thermal cycling responses of aged NiTiPd-10Hf polycrystalline shape memory alloy.

Plastic deformation is another mechanism that contributes hysteresis in SMAs.[24,25] Even though the alloy was weaker than the Ni-rich NiTi-20Hf and NiTi-20HfPd alloys,[6] it shows the ability of shape recovery against 700 MPa and higher recoverable strain than those alloys.[6]

Figure 4 shows the constant-temperature loading responses of the aged NiTiPd-10Hf alloy at selected temperatures. The samples were loaded incrementally till the selected strain levels at 70°C, 85°C and 110°C. The test temperatures were selected to be above A_f to observe fully superelastic responses. The initial linear regions in the curves represent elastic deformation of austenite followed by stress-induced austenite to martensite transformation (SIM). It is clear that high slopes were observed in the phase transformation regions in all the test temperatures. Upon unloading of the materials, back transformation from martensite to austenite was observed.

The critical stresses for SIM were 560 MPa, 714 MPa and 860 MPa for the test temperatures of 70°C, 85°C and 110°C, respectively. The

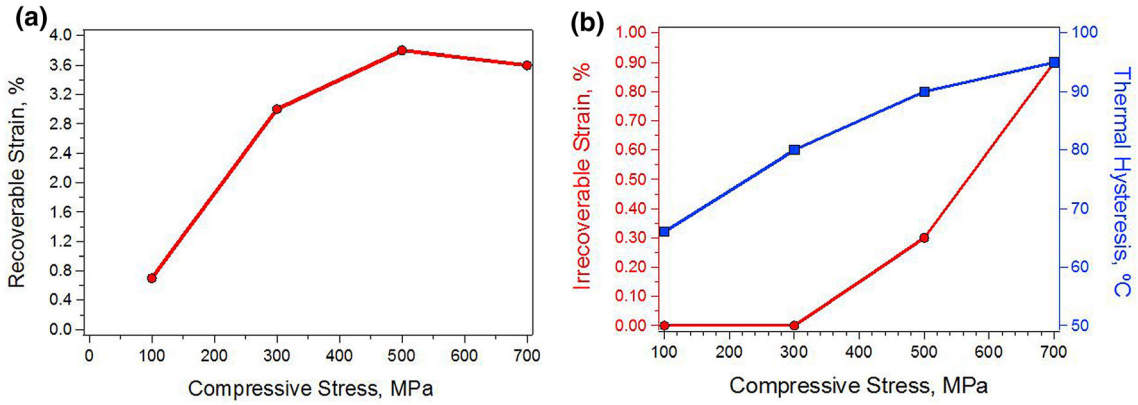

Fig. 3. (a) Recoverable strains (extracted from Fig. 2) and (b) irrecoverable strain and thermal hysteresis (extracted from Fig. 2) as a function of applied compressive stresses.

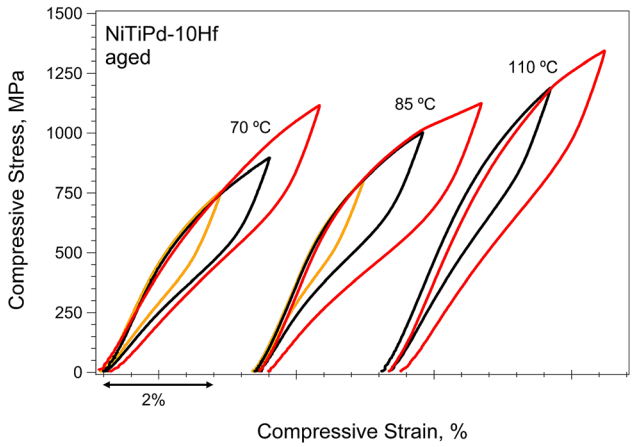

Fig. 4. Superelastic responses of the aged NiTiPd-10Hf polycrystalline shape memory alloy at selected test temperatures.

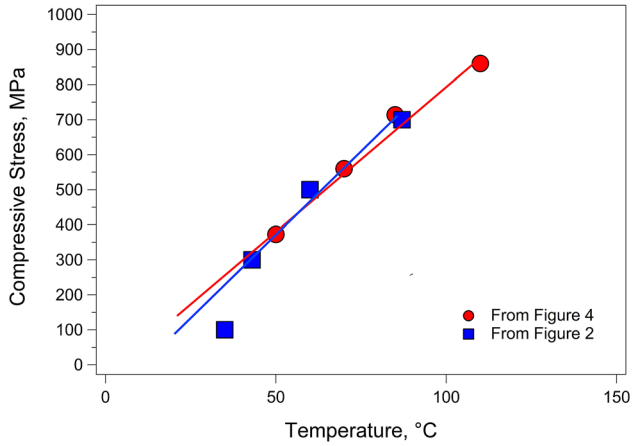

Fig. 5. Change in Ms with applied stress from the constant-stress thermal cycling experiments (Fig. 2) and the change in critical stress vs. temperature from the superelastic responses (Fig. 4) of the aged-NiTiPd-10Hf alloy.

recoverable strain (applied strain-elastic strain) was 2.2% while the irrecoverable strain was 0.1% at 70°C after loading the material to 4%. As the test temperature increased to 110°C, the recoverable strain was 1.7% while the plastic strain was 0.3%. It is clear that the recoverable strain decreased as the test temperature increased. The increased critical stress for SIM (resulting in higher elastic strain) and plastic deformation could be possible reasons for the decrease.

Figure 5 shows the critical stress levels for stress induced martensite formation as a function of test temperature (extracted from Fig. 4) and the M_s temperatures measured at selected cycling stress levels (extracted from Fig. 2). It is clear that the results are in good agreement for both methods.

The critical stress levels increased with the test temperature while the M_s temperatures increased with the increasing cycling stress following the Clausius–Clapeyron (C–C) relationships. The C–C relationship can be expressed as:

$$\frac{\Delta\sigma}{\Delta T} = -\frac{\Delta H}{\varepsilon_{tr} T_0}$$

where the difference between critical stresses is $\Delta\sigma$, ΔT is the temperature difference, T_0 is the equilibrium temperature, and ε_{tr} is the transformation strain.[26] The C–C slope extracted from Fig. 2 was 9.5 MPa/°C while the slope extracted from Fig. 4 was 8.2 MPa/°C. However, it should be mentioned that when the recoverable strain (or applied stress) is low, the Ms temperature determined from Fig. 2 deviates from the linear relationship as the strain can only be detected if reoriented martensite is present in the sample. Thus, the C–C slope determined from Fig. 4 is more reliable. The C–C slopes for the as-received NiTiPd-10Hf alloys were 8.5 MPa/°C (extracted from constant-stress thermal cycling) and 9.2 MPa/°C (extracted from superelasticity curves).[17] It is clear that the slopes of the as-received and aged NiTiPd-10Hf alloys were

consistent. In comparison, the C–C slope was 10.7 MPa/°C for an extruded $Ni_{45,3}Ti_{29,7}Hf_{20}Pd_5$ alloys,[16] while it was 12 MPa/°C for $Ni_{50}Ti_{50}$ alloys[27] in compression.

Figure 6 shows the deformation response of the aged NiTiPd-10Hf alloy at 35°C. The specimen was loaded up to failure, which occurred at 2340 MPa with a strain of slightly over 13%. The specimen is expected to have a mixture of martensite and austenite phases at 35°C. Thus, region 1 shows elastic deformation of both phases. After the linear part, region 2 starts at 380 MPa. It should be noted that the regions in Fig. 7 were separated by using an intersection graphical method.

Region 2 shows the stress-induced martensitic transformation of the existing austenite in addition to re-orientation/de-twinning of existing martensite phase in the microstructure. Thus, there are two concurrently active deformation mechanisms in region 2. It should be noted that plastic deformation could take place in local regions of the microstructure depending on the accumulated stresses and yielding stress in specific regions.

At the end of region 2, the material is expected to have a fully martensitic structure after both the stress-induced martensitic transformation and re-orientation/de-twinning processes. Thus, in region 3 elastic deformation of martensite is dominant in addition to localized plastic deformation by dislocation slip.

Region 4 starts with the second yield (2080 MPa) point where plastic deformation and/or deformation twinning of martensite is expected to be highly dominant. This region ended with the failure of the bulk aged NiTiPd-10Hf alloy. The aged NiTiPd-10Hf alloy failed at 2340 MPa with a compressive strain > 13%. The strength and ductility of the alloy are remarkable. It should be noted that Ni-rich NiTi-20Hf and $Ni_{45.3}Ti_{29,7}Hf_{20}Pd_5$ alloys were brittle because of the high Hf content.[17]

Figure 7 shows the work-out values of the as-received and aged NiTiPd-10Hf alloys. The work-out values were calculated by a mathematical multiplication of applied stress and recoverable strains shown in Fig. 2. It is clear that the work output levels increased with the applied stress owing to the increased recoverable strains. The work outputs were 7 J/cm^3 and 25.2 J/cm^3 against 100 MPa and 700 MPa, respectively. The maximum work output in the as-received NiTiPd-10Hf was 29 J/cm^3.[17] The reason in the difference of the maximum work output levels is strongly linked to the decreased recoverable strain in the aged alloy as mentioned earlier in the text.

The aged NiTiPd-10Hf alloy has comparable work output to the previously examined as-received NiTiPd-10Hf alloy, but lower compared to the $Ni_{45,3}Ti_{29,7}Hf_{20}Pd_5$ polycrystalline alloy, which is in the range 32–35 J/cm^3.[16] On the other hand, Ni-rich NiTiHf alloys can generate work outputs around 18–20 J/cm^3,[28] while the work output levels of binary NiTi alloys are in the range of 10–20 J/cm^3.[29]

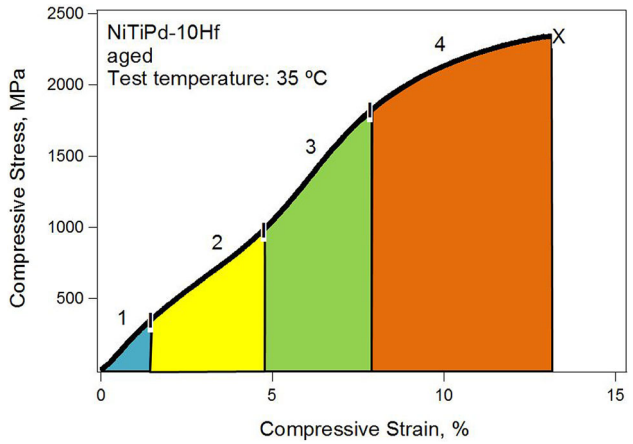

Fig. 6. Deformation response of the aged NiTiPd-10Hf alloy at 35°C.

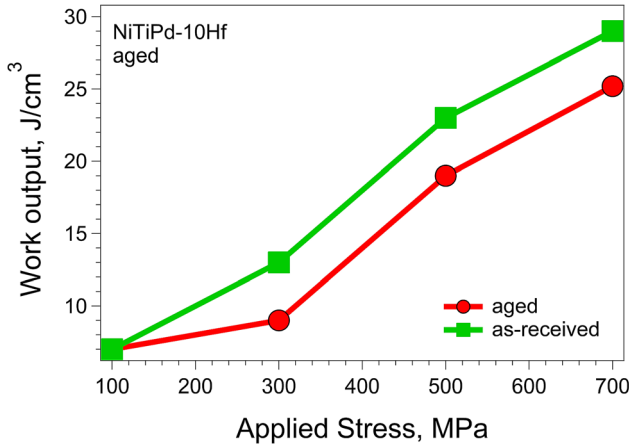

Fig. 7. Work output levels as a function of applied stress in the aged and as-received NiTiPd-10Hf alloy (data for the as-received material was taken from Ref.[16] for comparison).

Table I shows selected properties of NiTiHfPd alloys for comparison. It is clear that chemical composition and aging conditions have significant effects on properties.

In general, the aged NiTiPd-10Hf alloys showed a good shape memory effect and superelasticity. It should be noted that the $Ni_{45.3}Ti_{39.7}Hf_{10}Pd_5$ polycrystalline alloys were weaker compared to Ni-rich NiTi-20Hf and $Ni_{45.3}Ti_{29.7}Hf_{20}Pd_5$ polycrystalline alloys,[16] but had higher ductility and less expensive production costs. The aging of $Ni_{45.3}Ti_{39.7}Hf_{10}Pd_5$ polycrystalline alloys did not significantly alter the shape memory properties because of the low volume fraction of precipitates. This shows the importance of precipitate characteristics (volume fraction, precipitate size and inter-particle distance, etc.) on the properties of NiTiHf-based shape memory alloys. However, alternative methods such as rolling, aging at different temperatures and times, etc., could be

Table I. Selected properties of NiTiHfPd polycrystalline shape memory alloys

Alloy	Aging	Max. SME strain,%	Max. SE strain,%	Work output, MPa	References
$Ni_{45,3}Ti_{39,7}Pd_5$-Hf_{10}	550°C-3 h	4.6	2.2	29	This study
$Ni_{45,3}Ti_{39,7}Pd_5$-Hf_{10}	As-received	4.6	4.0	29	17
$Ni_{45,3}Ti_{34,7}Pd_5$-Hf_{15}	As-received	3.0	4.7	30	13
$Ni_{45,3}Ti_{29,7}Pd_5$-Hf_{20}	550°C-3 h	1.68	2.4	30	16

SME shape memory effect, *SE* super-elasticity

employed to further improve the shape memory and mechanical properties of low Hf content NiTiHfPd alloys.

CONCLUSION

Characterization of a $Ni_{45.3}Ti_{39.7}Hf_{10}Pd_5$ polycrystalline shape memory alloy after aging at 550°C for 3 h was conducted through microstructural and mechanical experiments. Based on the results, the following conclusions can be drawn. Aging the alloy at 550°C for 3 h did not result in high volume fraction precipitate formation in the microstructure. Thus, the related shape memory properties such as strength and TTs were not notably affected. The aged alloy showed 3.8% recoverable strain under 500 MPa in addition to superelastic recovery of 4% applied strain at the test temperature of 70°C. The C–C slope calculated from the constant-stress temperature cycling experiments was about 9.5 MPa/°C. The alloy failed at 2340 MPa with compressive strain > 13%. Further studies such as aging at different temperatures for longer hours could be conducted to check whether the volume fraction of coherent precipitates can be increased in the microstructure. On the other hand, forming methods such as extrusion or rolling might be employed to increase the strength of the Ni45.3Ti39.7Hf10Pd5 polycrystalline alloy to help improve shape memory properties.

ACKNOWLEDGEMENTS

This work was supported in part by NSF CMMI-15-38665, the NASA EPSCOR program, under Grant No. NNX11AQ31A and the KY EPSCoR RID program under grant no. 3049024332.

CONFLICT OF INTEREST

The authors declare that they have no conflict of interest.

REFERENCES

1. K. Otsuka and X. Ren, *Prog. Mater Sci.* 50, 511 (2005).
2. J. Ma, I. Karaman, and R.D. Noebe, *Int. Mater. Rev.* 55, 257 (2010).
3. I. Kaya, H. Tobe, H.E. Karaca, E. Acar, and Y. Chumlyakov, *Acta Metallurgica Sinica (English Letters)* 29, 282 (2016).
4. S. Besseghini, E. Villa, and A. Tuissi, *Mater. Sci. Eng., A* 273–275, 390 (1999).
5. D. R. Angst, P. E. Thoma and M. Y. Kao, J. Phys. IV France, 05 (C8), C8-747-C748-752 (1995).
6. H.E. Karaca, E. Acar, H. Tobe, and S.M. Saghaian, *Mater. Sci. Technol.* 30, 1530 (2014).
7. S. Padula, S. Qiu, D. Gaydosh, R. Noebe, G. Bigelow, A. Garg, and R. Vaidyanathan, *Metall. Mater. Trans. A* 43, 4610 (2012).
8. E. Acar, M. Çalışkan, and H.E. Karaca, *Appl. Phys. A* 125, 239 (2019).
9. H.E. Karaca, E. Acar, G.S. Ded, S.M. Saghaian, B. Basaran, H. Tobe, M. Kok, H.J. Maier, R.D. Noebe, and Y.I. Chumlyakov, *Mater. Sci. Eng., A* 627, 82 (2015).
10. H.Y. Kim, T. Jinguu, T.-H. Nam, and S. Miyazaki, *Scripta Mater.* 65, 846 (2011).
11. K.C. Atli, I. Karaman, R.D. Noebe, A. Garg, Y.I. Chumlyakov, and I.V. Kireeva, *Acta Mater.* 59, 4747 (2011).
12. S.F. Hsieh and S.K. Wu, *Mater. Charact.* 45, 143 (2000).
13. E. Acar, H. Tobe, I. Kaya, H.E. Karaca, and Y.I. Chumlyakov, *J. Mater. Sci.* 50, 1924 (2015).
14. E. Acar, *Mater. Sci. Eng., A* 633, 169 (2015).
15. E. Acar, H.E. Karaca, H. Tobe, R.D. Noebe, and Y.I. Chumlyakov, *Intermetallics* 54, 60 (2014).
16. H.E. Karaca, E. Acar, G.S. Ded, B. Basaran, H. Tobe, R.D. Noebe, G. Bigelow, and Y.I. Chumlyakov, *Acta Mater.* 61, 5036 (2013).
17. E. Acar, H.E. Karaca, H. Tobe, R.D. Noebe, and Y.I. Chumlyakov, *J. Alloys Compd.* 578, 297 (2013).
18. E. Acar, H. Tobe, H.E. Karaca, and I. Chumlyakov, *Mater. Sci. Eng., A* 725, 51 (2018).
19. G.P. Toker, S. Saedi, E. Acar, O. Ozbulut, and H.E. Karaca, *J. Alloys Compd.* 763, 1012 (2018).
20. D. R. Coughlin, *Ohio State University, Ohio*, 2013.
21. H.E. Karaca, S.M. Saghaian, G. Ded, H. Tobe, B. Basaran, H.J. Maier, R.D. Noebe, and Y.I. Chumlyakov, *Acta Mater.* 61, 7422 (2013).
22. Y.I. Chumlyakov, E.Y. Panchenko, I.V. Kireeva, S.P. Efimenko, V.B. Aksenov, and H. Sehitoglu, *Dokl. Phys.* 47, 510 (2002).
23. M. Nishida, C.M. Wayman, and A. Chiba, *Metallography* 21, 275 (1988).
24. R.F. Hamilton, H. Sehitoglu, Y. Chumlyakov, and H.J. Maier, *Acta Mater.* 52, 3383 (2004).
25. H. Sehitoglu, R. Hamilton, H.J. Maier, and Y. Chumlyakov, *J. Phys. IV France* 115, 3 (2004).
26. P. Wollants, J.R. Roos, and L. Delaey, *Prog. Mater Sci.* 37, 227–288 (1993).
27. L. Orgéas and D. Favier, *Acta Mater.* 46, 5579 (1998).
28. H.E. Karaca, S.M. Saghaian, B. Basaran, G.S. Bigelow, R.D. Noebe, and Y.I. Chumlyakov, *Scripta Mater.* 65, 577 (2011).
29. D.S. Grummon, *JOM* 55, 24 (2003).